Cellular/Molecular

G-Proteins Modulate Cumulative Inactivation of N-Type (Ca$_V$2.2) Calcium Channels

Sarah McDavid[1] and Kevin P. M. Currie[1,2,3]

Departments of [1]Anesthesiology and [2]Pharmacology, and [3]Center for Molecular Neuroscience, Vanderbilt University Medical Center, Nashville, Tennessee 37232

Precise regulation of N-type (Ca$_V$2.2) voltage-gated calcium channels (Ca-channels) controls many cellular functions including neurotransmitter and hormone release. One important mechanism that inhibits Ca^{2+} entry involves binding of G-protein $\beta\gamma$ subunits (G$\beta\gamma$) to the Ca-channels. This shifts the Ca-channels from "willing" to "reluctant" gating states and slows activation. Voltage-dependent reversal of the inhibition (facilitation) is thought to reflect transient dissociation of G$\beta\gamma$ from the Ca-channels and can occur during high-frequency bursts of action potential-like waveforms (APW). Inactivation of Ca-channels will also limit Ca^{2+} entry, but it remains unclear whether G-proteins can modulate inactivation. In part this is because of the complex nature of inactivation, and because facilitation of Ca-channel currents (I_{Ca}) masks the extent and kinetics of inactivation during typical stimulation protocols. We used low-frequency trains of APW to activate I_{Ca}. This more closely mimics physiological stimuli and circumvents the problem of facilitation which does not occur at ≤5 Hz. Activation of endogenous G-proteins reduced both Ca^{2+}-dependent, and voltage-dependent inactivation of recombinant I_{Ca} in human embryonic kidney 293 cells. This was mimicked by expression of wild-type G$\beta\gamma$, but not by a point mutant of G$\beta\gamma$ with reduced affinity for Ca-channels. A similar decrease in the inactivation of I_{Ca} was produced by P2Y receptors in adrenal chromaffin cells. Overall, our data identify and characterize a novel effect of G-proteins on I_{Ca}, and could have important implications for understanding how G-protein-coupled receptors control Ca^{2+} entry and Ca^{2+}-dependent events such as neurotransmitter and hormone release.

Key words: calcium current; G-protein; patch clamp; inactivation; neuromodulation; GPCR; N-type; calcium; inhibition

Introduction

Precise regulation of Ca^{2+} entry through N-type voltage-gated calcium channels (Ca-channels) controls many cellular functions including neurotransmitter and hormone release. One important inhibitory mechanism involves binding of G-protein $\beta\gamma$ subunits (G$\beta\gamma$) to the Ca-channels (for review, see Ikeda and Dunlap, 1999; Dolphin, 2003; Elmslie, 2003; De Waard et al., 2005). Models envision that G$\beta\gamma$ shifts the Ca-channels from "willing" to "reluctant" gating states and slows activation (Bean, 1989; Elmslie et al., 1990; Boland and Bean, 1993; Golard and Siegelbaum, 1993; Colecraft et al., 2000; Lee and Elmslie, 2000). A defining feature of G$\beta\gamma$-mediated inhibition is reversal by a strongly depolarizing voltage-step (Bean, 1989; Elmslie et al., 1990; Penington et al., 1991). This reversal (facilitation) is thought to reflect transient dissociation of G$\beta\gamma$ from the Ca-channels at depolarized membrane potentials. Modest facilita-

tion can also occur during high-frequency bursts of action potentials, and might contribute to short-term synaptic plasticity (Womack and McCleskey, 1995; Brody et al., 1997; Williams et al., 1997; Park and Dunlap, 1998; Tosetti et al., 1999; Currie and Fox, 2002).

Inactivation of Ca-channels also limits Ca^{2+} entry during sustained or repetitive stimuli. However, the effects (if any) of G-proteins on inactivation of I_{Ca} remain unclear. In part this is because facilitation partially masks the extent and kinetics of inactivation during typical stimulation protocols. Furthermore, there are several components to voltage-dependent inactivation (VDI) (Jones and Marks, 1989; Patil et al., 1998), and at least one form of Ca^{2+}-dependent inactivation (CDI) (Cox and Dunlap, 1994; Liang et al., 2003; Goo et al., 2006). The kinetics and perhaps the dominant "component" of inactivation might vary with the pattern of stimulation. For example, during trains of action potential-like waveforms (APW), inactivation occurs preferentially from intermediate closed state(s) of the channel (Patil et al., 1998).

It has been suggested that G$\beta\gamma$ might accelerate inactivation of I_{Ca} during high-frequency trains of APW by increasing the probability that Ca-channels occupy the closed state(s) from which they preferentially inactivate (Patil et al., 1998). However, this has not been rigorously tested and single channel recording found little effect of G$\beta\gamma$ on inactivation (Meir and Dolphin, 2002). Other circumstantial evidence provides hints that

G-proteins could potentially modulate inactivation. Specifically, the intracellular loop connecting domains I and II on the α_1-subunit of Ca-channels (I–II loop) is the primary binding site for $G\beta\gamma$ (De Waard et al., 1997; Herlitze et al., 1997). The I–II loop might also constitute the "gate" for fast inactivation (Restituito et al., 2000; Stotz et al., 2000; Stotz and Zamponi, 2001; Geib et al., 2002; Cens et al., 2006), raising the possibility that $G\beta\gamma$ might disrupt movement or interaction of this putative "inactivation gate" with other channel domains.

In this study, we show that $G\beta\gamma$ reduces both voltage-dependent and calcium-dependent inactivation of I_{Ca} during trains of APW. Reduced inactivation could alter the time course of Ca^{2+} entry, and diminish the "efficacy" of $G\beta\gamma$-mediated inhibition of I_{Ca} during sustained trains of APW. These findings could have important implications for understanding how G-proteins control Ca^{2+}-dependent events such as neurotransmitter and hormone release.

Materials and Methods

Cell culture and transfection. Human embryonic kidney 293 (HEK293) cells stably expressing N-type Ca^{2+} channels [α_{1B} ($Ca_{V2.2}$), β_{1b}, and α_2d subunits] (McCool et al., 1996, 1998) were kindly provided by Dr Heidi Hamm (Vanderbilt University, Nashville, TN). Cells were grown in MEM supplemented with fetal bovine serum (10%), glutamine (2 mM), penicillin/streptomycin (100 U/ml/100 g/ml), and G418 (0.5 mg/ml). Cells were maintained in an incubator (37°C in 95% air and 5% CO_2 at ~90% humidity) and passaged every 3–5 d for up to ~25 passages. Cells were replated onto poly-lysine-coated glass coverslips for patch-clamp recording. Transfection of cells with Qiagen (Valencia, CA) purified plasmids was performed using lipofectamine 2000 (Invitrogen, Grand Island, NY) in 35 mm tissue culture dishes as per manufacturer instructions. Cells were transfected with both EGFP-tagged $G\beta_1$ and $G\gamma_2$ subunits (1:2 ratio). In some cells, we used a point mutant of $G\beta_1$ (W332A-$G\beta_1$) along with Gγ2. Control cells were transfected with EGFP alone. All plasmids were kindly provided by Eun-Ja Yoon and Dr. Heidi Hamm (Vanderbilt University). Recording was performed ~48–72 h after transfection on cells that had been replated on poly-lysine-coated glass coverslips for ~12–24 h. Transfected cells were visually identified using fluorescence of EGFP.

Adult bovine adrenal glands were obtained from a local slaughterhouse and chromaffin cells were prepared by digestion with collagenase followed by density gradient centrifugation based on previously published protocols (Fenwick et al., 1978; Greenberg and Zinder, 1982). The cells were plated onto coverslips coated with collagen (at a density of ~0.2×10^6 cell/ml). Cells were maintained in an incubator at 37°C in an atmosphere of 95% air and 5% CO_2 with a relative humidity of ~90%. Fibroblasts were effectively suppressed with cytosine-arabinoside (10 μM) (Sigma-Aldrich; St. Louis, MO), leaving relatively pure chromaffin cell cultures. Half of the culture medium was exchanged every day. This medium consisted of DMEM12 (1:1) supplemented with fetal bovine serum (10%), glutamine (2 mM), penicillin/streptomycin (100 U/ml^{-1}/ 100 g/ml^{-1}), cytosine arabinoside (10 μM), and 5-fluorodeoxyuridine (10 μM). Chromaffin cells were recorded from 2–5 d after cell isolation.

Electrophysiology. For experiments on recombinant channels in HEK293 cells, calcium channel currents (I_{Ca}) were recorded in the standard whole-cell patch-clamp recording configuration using a Molecular Devices (Union City, CA) Axopatch 200B amplifier and custom software written in Axobasic or VisualBasic (kindly provided by Dr. Aaron Fox, University of Chicago, Chicago, IL). Data were filtered at 2 kHz and sampled every 20–100 μs. Analyses were performed using custom written programs, Synaptosoft (Decatur, GA) Mini Analysis program, and OriginPro software. Electrodes were pulled from microhematocrit capillary tubes (Fisher Scientific, Houston, TX) and coated with Sylgard (Dow Corning, Midland, MI). After fire polishing, electrodes had resistances of <2 MΩ. Series resistance was partially compensated using the Axopatch circuitry. The recording bath (total volume, ~250–300 μl) was continually washed with fresh extracellular solution at a rate of ~4

ml/min from gravity-fed reservoirs. The APW used to stimulate cells (see Fig. 1A) is based on a current-clamp recording of an action potential from an adrenal chromaffin cell at room temperature (Currie and Fox, 2002). Data were subjected to linear leak and capacitance subtraction before quantitative analysis, and presented as mean ± SE. The percent inactivation at the end of a train of APW for each cell was determined by taking the mean percent decrease in current amplitude of the last three pulses within a train relative to the first pulse within the same train. Statistical analysis was performed using Student's *t* test (paired or independent as appropriate). All recordings were performed at room temperature.

In experiments with chromaffin cells, I_{Ca} was recorded in the perforated whole-cell recording configuration. The pipette tip was filled with amphotericin-free solution and then backfilled with solution that contained ~0.5 mg/ml amphotericin-B (Calbiochem, La Jolla, CA). After forming a cell attached seal, series resistance was monitored to assess the progress of perforation. Typically, series resistance <10–15 MΩ was achieved within 5–15 min and cells that did not show good perforation within this time frame were discarded.

Drugs and solutions. Unless noted otherwise, all reagents were from Sigma-Aldrich. For standard whole-cell recording, the patch-pipette solution consisted of the following (in mM): 125 CsCl, 4 MgCl$_2$, 20 HEPES, 0.3 EGTA, 0.35 GTP, 4 ATP, 14 creatine phosphate, pH 7.3, ~310 mOsm. Where indicated in the results section, the concentration of EGTA was increased from 0.3 to 10 mM (see Fig. 1). In a few experiments, EGTA was replaced with 5 mM BAPTA. Also, where indicated, the patch-pipette solution contained ~70 μM GTP-γ-S to directly activate endogenous G-proteins and elicit inhibition of I_{Ca}. The extracellular NaCl-based solution used to bathe cells before and during seal formation consisted of the following (in mM): 145 NaCl, 2 KCl, 1 MgCl$_2$, 10 glucose, 10 HEPES, 2 CaCl$_2$, pH 7.3, osmolarity ~315 mOsm. After entering the whole-cell recording configuration the bath solution was switched to one containing the following (in mM): 155 tetraethylammonium Cl, 10 glucose, 10 HEPES, 5 or 10 CaCl$_2$, pH 7.3, 320–330 mOsm. Where indicated, Ca^{2+} was replaced with Ba^{2+} in the extracellular solution to minimize calcium-dependent inactivation of I_{Ca}. Our preliminary data (not shown) confirmed previous reports that this shifts the current–voltage relationship by ~10 mV (Liang and Elmslie, 2001). Thus, when using Ba^{2+}-containing recording solutions, the APW was adjusted to peak at +35 mV rather than +45 mV. ω-Conotoxin GVIA was from Alomone Labs (Jerusalem, Israel) and stocks (100–300 μM) were prepared in sterile H_2O and frozen until use. Conotoxin was applied to cells by bolus application to a static bath as described in the results section (see Fig. 6).

For perforated recordings in chromaffin cells, the patch-pipette solution consisted of the following (in mM): 145 Cs-glutamate; 10 HEPES; 9.5 NaCl; 0.5 tetraethylammonium-Cl. Amphotericin stocks (50 mg/ml in DMSO) were refrigerated protected from light for up to 3 d. Working solutions (~0.5 mg/ml) were prepared shortly before use by addition to patch-pipette solution and sonication. The extracellular solution for chromaffin cell recording consisted of the following (in mM): 150 NaCl, 2 KCl, 2 MgCl$_2$, 10 glucose, 10 HEPES, 2 CaCl$_2$, 0.05–0.1 TTX, 0.01 nitrendipine, pH 7.3, osmolarity ~315 mOsm.

Results

Both voltage-dependent and calcium-dependent inactivation control N-type Ca-channels during a train of action potential-like stimuli

There has been considerable debate as to whether CDI controls N-type I_{Ca} (Jones and Marks, 1989; Cox and Dunlap, 1994; Patil et al., 1998; Goo et al., 2006). Recombinant Ca-channels expressed in HEK293 cells do display CDI, at least when VDI was minimized by coexpressing the β_{2a} subunit (Liang et al., 2003). However, it remains unclear whether CDI plays a significant role during stimuli that mimic trains of action potentials, especially in Ca-channels that also exhibit robust VDI. We used HEK293 cells stably expressing $Ca_{V2.2}$ (α_{1B}), β_{1b}, and $\alpha_2\delta$ subunits (McCool et al., 1996, 1998) to enable recording of currents from a single population of Ca-channels with defined subunit composition.
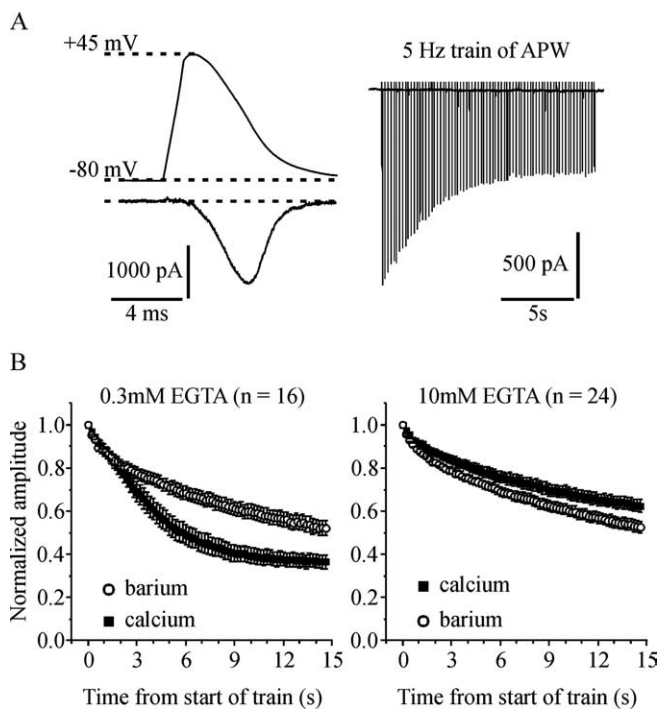
Figure 1. Both voltage-dependent and Ca^{2+}-dependent inactivation of I_{Ca} play a significant role during a sustained train of APW. **A,** The top left shows the APW used to stimulate the cells, and the bottom left shows a representative I_{Ca}. The right panel shows a series of I_{Ca} elicited by a train of APW applied at 5 Hz for 15 s. **B,** Cells were stimulated with a 5 Hz train of APW first in extracellular solution containing 5 mM Ca^{2+} and then in solution containing 5 mM Ba^{2+}. Peak current amplitude elicited by each APW was normalized to the first pulse within the train and plotted against time. The left panel shows data from cells recorded with 0.3 mM EGTA in the patch-pipette solution. The decline in current amplitude during the train was significantly greater in Ca^{2+} than in Ba^{2+} ($p < 0.0001$) indicating that Ca^{2+}-dependent inactivation plays a role. The right panel is from cells recorded with 10 mM EGTA in the patch-pipette solution. The decline in current amplitude during the train was slightly but significantly less in Ca^{2+} than in Ba^{2+} ($p < 0.002$). Error bars indicate SEM.

Ca-channels containing the β_{1b} subunit are known to exhibit robust VDI (Yasuda et al., 2004).

Cells were stimulated with an APW based on an action potential recorded from an adrenal chromaffin cell at room temperature (Currie and Fox, 2002). Chromaffin cells typically fire at lower frequencies like those used in this study (<25 Hz). An example of a Ca-channel current (I_{Ca}) elicited by this APW is illustrated in Figure 1A. Stimulating cells with a train of 75 APW applied at 5 Hz produced a robust decrease in I_{Ca} amplitude (inactivation) during the first ∼6–8 s of the train (Fig. 1A, right). The amplitude of I_{Ca} recovered (≥90%) in the 1–2 min after the end of the APW train (data not shown). To determine whether CDI contributed to the decrease in current amplitude, we replaced extracellular Ca^{2+} with Ba^{2+}. Calcium-dependent inactivation is mediated by calmodulin (Liang et al., 2003) and is poorly supported by Ba^{2+}. Cells with low intracellular calcium buffering (0.3 mM EGTA in the patch-pipette) were stimulated with a 5 Hz train of APW first in Ca^{2+}-containing extracellular solution and then in Ba^{2+}-containing solution. The decline in peak current amplitude was significantly greater with Ca^{2+} present than with Ba^{2+} (63 ± 3% in Ca^{2+} vs 48 ± 3% in Ba^{2+}; $n = 16$; $p < 0.0001$) (Fig. 1B, left), demonstrating a contribution of CDI.

We repeated the same experiment but with 10 mM EGTA in the patch-pipette. Under these conditions, CDI was abolished because the decline in current amplitude during the APW train

was not increased in Ca^{2+}-containing compared with Ba^{2+}-containing extracellular solution. Indeed, the decline in current amplitude was significantly less in Ca^{2+} than in Ba^{2+} (37 ± 3% in Ca^{2+} vs 47 ± 3% in Ba^{2+}; $n = 24$; $p < 0.002$) (Fig. 1B, right). We also recorded from cells with 5 mM BAPTA in the patch-pipette solution. Under these conditions, the decline in current amplitude was not significantly different in Ca^{2+} compared with Ba^{2+} (41 ± 7% in Ca^{2+} vs 36 ± 6% in Ba^{2+}; not significant, $p = 0.26$; $n = 6$).

Overall, these data support a previous report showing that higher concentrations of intracellular EGTA can prevent CDI of recombinant N-type channels (Liang et al., 2003). In addition, we show that both voltage-dependent inactivation and calcium-dependent inactivation are functionally relevant for the control of N-type I_{Ca} during trains of APW.

G-proteins reduce inactivation of I_{Ca} during low-frequency trains of APW

The endogenous somatostatin receptors in HEK cells couple to exogenously expressed Ca-channels, but this response desensitizes during prolonged agonist application. This desensitization would confound interpretation of our data during sustained trains of APW. To circumvent this problem, we included GTP-γ-S in the patch-pipette solution, which leads to essentially irreversible activation of G-proteins and tonic inhibition of I_{Ca}. In all experiments (both control and with GTP-γ-S), we waited at least 5 min after entering the whole-cell recording configuration to ensure there was ample time for the patch-pipette solution to diffuse into and equilibrate with the intracellular milieu. A defining feature of G$\beta\gamma$-mediated inhibition of I_{Ca} is reversal by a strongly depolarizing voltage step (Bean, 1989; Elmslie et al., 1990; Penington et al., 1991). This reversal, termed prepulse facilitation, is thought to be caused by transient dissociation of G$\beta\gamma$ from the channel at the depolarized membrane potential. Functionally, prepulse facilitation is indicative of the extent of G$\beta\gamma$-mediated inhibition of I_{Ca}. We determined the prepulse facilitation ratio (current amplitude with a prepulse normalized to that without a prepulse) in each cell to confirm tonic inhibition of I_{Ca} attributable to activation of endogenous G-proteins by GTP-γ-S (Fig. 2A). Controls cells showed little or no facilitation (1.12 ± 0.03; $n = 21$) whereas cells with GTP-γ-S showed robust facilitation (1.77 ± 0.09; $n = 24$; $p < 0.0001$). High-frequency bursts of action potential-like stimuli can also produce modest facilitation of I_{Ca} caused by reversal of G$\beta\gamma$-mediated inhibition (Womack and McCleskey, 1995; Brody et al., 1997; Williams et al., 1997; Park and Dunlap, 1998; Tosetti et al., 1999; Currie and Fox, 2002). To avoid this complication, we used low-frequency trains of APW (5 Hz) that we have shown previously do not produce facilitation (Currie and Fox, 2002).

Control cells (no GTP-γ-S) or cells with GTP-γ-S in the patch-pipette solution were stimulated with a 5 Hz train of APW lasting 15 s. As expected, the initial amplitude of I_{Ca} was smaller in cells with GTP-γ-S because of tonic G$\beta\gamma$-mediated inhibition of the Ca-channels (1426 ± 201 pA in control cells vs 671 ± 99 pA in GTP-γ-S cells; $p < 0.01$) (Fig. 2B). Our data also reveal an additional, novel effect: inactivation of I_{Ca} (decrease in amplitude) during the train of APW was significantly reduced by GTP-γ-S (Fig. 2B,C). Consequently, after ∼6–8 s of stimulation, the amplitudes of I_{Ca} in control cells and GTP-γ-S cells converge and are not significantly different.

As already shown (Fig. 1B), CDI and VDI both contribute to the decline in amplitude of I_{Ca} during a train of APW. To determine whether G-proteins targeted VDI, CDI, or both forms of
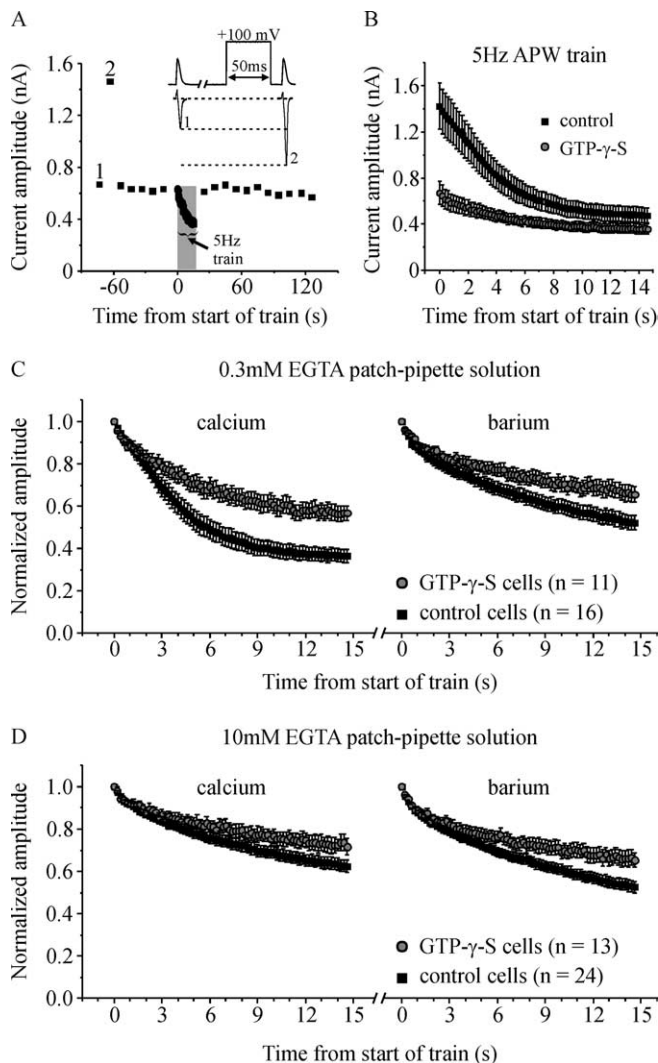
Figure 2. Activation of endogenous G-proteins reduces inactivation of I_{Ca}. **A**, Peak current amplitude is plotted against time from a representative cell recorded with GTP-γ-S in the patch-pipette solution. Time 0 is set at the start of the 5 Hz APW train. The data shown commenced ~6 min after entering the whole-cell recording configuration to allow time for GTP-γ-S to diffuse into the cell and for the current amplitude to stabilize. The inset shows the voltage stimulus (top) and representative currents (bottom) corresponding to the numbered data points (1, 2). (Note that for display clarity, the outward current elicited by the prepulse is not shown.) The increase in I_{Ca} amplitude produced by the conditioning prepulse (current 2) (pre-pulse facilitation) is caused by reversal of tonic Gβγ-mediated inhibition and confirmed activation of G-proteins by GTP-γ-S. A 5 Hz train of APW lasting 15 s produced robust inactivation of I_{Ca} that rapidly recovered after the end of the train. **B**, Peak amplitude of I_{Ca} elicited by a 5 Hz train of APW is plotted against time for control cells and cells with GTP-γ-S in the patch pipette. Cells were recorded in Ca^{2+}-containing extracellular solution. **C**, Control cells or cells with GTP-γ-S in the patch pipette were stimulated with a 5 Hz train of APW first in Ca^{2+}-containing extracellular solution, and then in Ba^{2+}-containing extracellular solution. Current amplitude was normalized to the first pulse within the train and plotted against time. All cells were recorded with 0.3 mM EGTA in patch-pipette solution. GTP-γ-S significantly reduced inactivation (the decline in current amplitude) in both Ca^{2+}- ($p < 0.001$) and Ba^{2+}- ($p < 0.02$) containing solutions. **D**, Same layout as in **C** except cells were recorded with 10 mM EGTA in the patch-pipette solution rather than 0.3 mM. GTP-γ-S significantly reduced inactivation in both Ca^{2+}- ($p < 0.04$) and Ba^{2+}- ($p < 0.01$) containing solutions. Error bars indicate SEM.

Figure 3. G-protein βγ subunits reduce inactivation of I_{Ca}. Cells were transiently transfected with $Gγ_2$ and either wild-type $Gβ_1$ or a point mutant (W332A) of $Gβ_1$. The Gβ subunits were tagged with EGFP to enable visual identification of transfected cells. Control cells were transiently transfected with EGFP. **A**, Mean prepulse facilitation of I_{Ca} produced by a conditioning step to +100 mV is plotted. Cells transfected with wild-type Gβγ showed strong prepulse facilitation of I_{Ca} (*$p < 0.001$ compared with controls) because of reversal of tonic inhibition of I_{Ca}. In cells transfected with W332A-Gβγ, facilitation was not significantly different from control (EGFP) cells, confirming that W332A-Gβγ does not bind to and inhibit Ca-channels. **B**, Control cells and cells expressing wild-type Gβγ were stimulated with a 5 Hz train of APW in Ca^{2+}-containing and then in Ba^{2+}-containing recording solutions. Current amplitude was normalized to the first APW of the train and plotted against time. Wild-type Gβγ significantly reduced inactivation compared with control cells in both Ca^{2+} ($p < 0.003$) and Ba^{2+} ($p < 0.04$) recording solutions. **C**, Same layout as **B** but comparing control cells and cells expressing W332A-Gβγ. Inactivation was not significantly reduced by W332A-Gβγ. Error bars indicate SEM.

which we have shown prevents CDI (Fig. 1). Under these conditions, with CDI blocked, GTP-γ-S still significantly reduced VDI in both Ca^{2+} ($p < 0.04$) and in Ba^{2+}-containing solutions ($p < 0.01$) (Fig. 2D). Together, these data confirm that at least some of the effect of G-proteins is on VDI. Our data also suggest that CDI is targeted, because the effect of G-proteins is greatest when both CDI and VDI are functional (0.3 mM EGTA with extracellular Ca^{2+}) (Fig. 2C).

G-protein βγ subunits (Gβγ) reduce the inactivation of I_{Ca}, perhaps through a direct interaction with the channel

To determine whether Gβγ signaling underlies the effect of G-proteins on inactivation of I_{Ca}, we transiently transfected cells with EGFP-tagged $Gβ_1$ and $Gγ_2$ (Gβγ) (Fig. 3A,B). EGFP-

inactivation, we minimized CDI by replacing extracellular Ca^{2+} with Ba^{2+}. In Ba^{2+}-containing extracellular solution GTP-γ-S still significantly reduced inactivation although the magnitude of the effect was smaller than in Ca^{2+} (Fig. 2C, right). In another approach, we used 10 mM EGTA in the patch-pipette solution
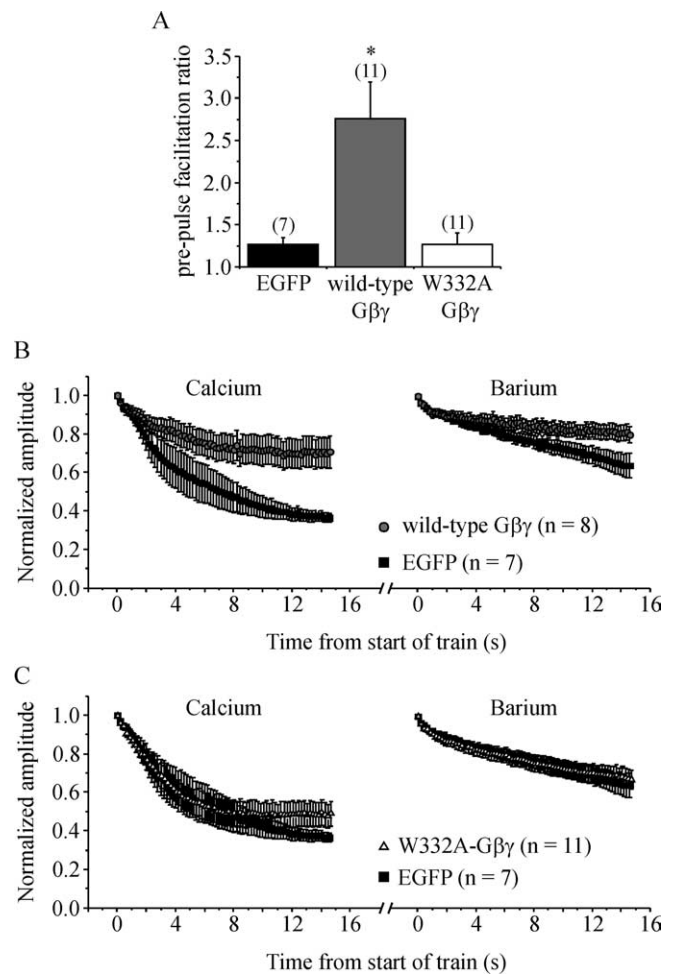
expressing cells were visually selected for patch-clamp recording and most displayed strong prepulse facilitation of I_{Ca} (Fig. 3A). Prepulse facilitation was attributable to reversal of tonic I_{Ca} inhibition and confirmed functional expression of G$\beta\gamma$ dimers. Note that three of 11 cells transfected with G$\beta\gamma$ showed little or no facilitation, likely reflecting poor expression of the Gγ subunit (E.-J. Yoon and K. Currie, unpublished observation). Control cells were transfected with EGFP alone and displayed minimal prepulse facilitation that was not significantly different from nontransfected cells.

We compared inactivation of I_{Ca} during a 5 Hz train of APW in G$\beta\gamma$-transfected cells and control (EGFP transfected) cells. Cells transfected with G$\beta\gamma$ that showed prepulse facilitation of I_{Ca} ($n = 8$) displayed significantly less inactivation during a 5 Hz train of APW in both Ca^{2+} ($p < 0.003$) and Ba^{2+} recording solutions ($p < 0.04$) (Fig. 3B). Inactivation in the three cells transfected with G$\beta\gamma$ that did not show prepulse facilitation (i.e., G$\beta\gamma$ was not functionally expressed) was identical to that in EGFP-transfected control cells (data not shown).

Point mutations of Gβ_1 have been identified that selectively disrupt binding to different effectors (Ford et al., 1998). One such mutant, W332A-Gβ_1, disrupts inhibition of I_{Ca} by reducing the affinity with which G$\beta\gamma$ binds to the channel (Ford et al., 1998; Agler et al., 2003). Previous reports have shown that W332A-Gβ_1 folds normally, is expressed similarly to wild-type, and can still interact with some other G$\beta\gamma$ effectors (Ford et al., 1998). Prepulse facilitation of I_{Ca} in cells transfected with W332A-Gβ + Gγ (Fig. 3A) was not significantly different from EGFP-transfected control cells, confirming that this mutant does not bind to and inhibit Ca-channels. We also show that W332A-G$\beta\gamma$ did not significantly reduce inactivation of I_{Ca} during a 5 Hz train of APW ($n = 11$) (Fig. 3D). These data are consistent with the idea that G$\beta\gamma$ must bind to the Ca-channels to reduce inactivation of I_{Ca}.

Facilitation does not mask inactivation of I_{Ca} during low-frequency trains of APW

We propose that G$\beta\gamma$ reduces inactivation of I_{Ca} during a train of APW. However, if facilitation (reversal of G$\beta\gamma$-mediated inhibition) were to occur during the train of APW, it would mask the full extent of inactivation. The net effect would be that the decline in I_{Ca} amplitude would be reduced, although inactivation per se is not altered. Facilitation of I_{Ca} can occur during trains of APW, but only at higher-stimulation frequencies (Womack and McCleskey, 1995; Brody et al., 1997; Williams et al., 1997; Park and Dunlap, 1998; Tosetti et al., 1999; Currie and Fox, 2002). This is because the brief, moderate membrane depolarization during an APW causes only minimal facilitation of I_{Ca} (dissociation of G$\beta\gamma$ from the Ca-channels). When the membrane potential returns to resting levels, G$\beta\gamma$ will rebind to (and reinhibit) those channels. During repetitive stimulation, if full reinhibition does not occur before the next APW, then the residual facilitation will summate with each successive APW. Thus, cumulative facilitation is only observed when the interval between successive APW is short (i.e., higher-stimulation frequencies). At lower frequencies, summation does not occur and overall facilitation is negligible (Currie and Fox, 2002).

We have shown previously that facilitation does not occur during a train of 20 APW applied at 5 Hz (Currie and Fox, 2002). Nevertheless, we wanted to confirm that summation of facilitation is unlikely to occur under the recording conditions, and in the cells used for this study. To do so, we determined the rate with which G$\beta\gamma$ re-inhibits I_{Ca} after strong prepulse facilitation (Fig.
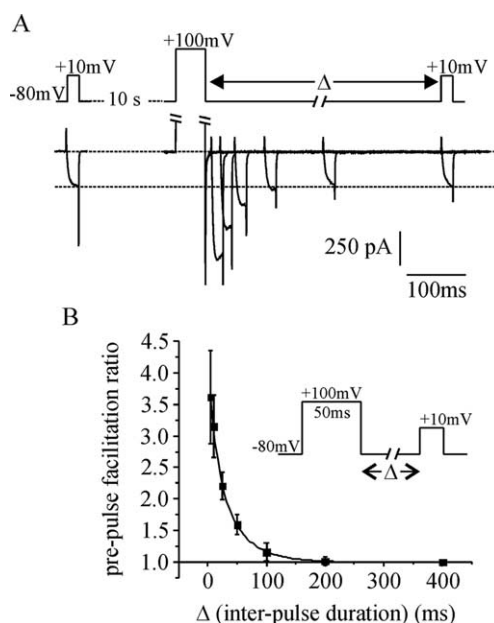

Figure 4. Reblock kinetics after prepulse facilitation of I_{Ca}. Cells were transfected with wild-type G$\beta_1\gamma_2$ (G$\beta\gamma$), and prepulse facilitation of I_{Ca} was recorded. **A**, The top shows the voltage commands, and the bottom shows six superimposed I_{Ca} recorded from a representative cell. The interval (Δ) between the prepulse and the test-pulse was varied with each sweep (10, 20, 50, 100, 200, and 400 ms). When the interval (Δ) was $\geq$100 ms, there was little or no facilitation of I_{Ca}. (Note that for display clarity, the outward current elicited by the prepulse and the largest of the inward tail currents have been clipped.) **B**, Mean prepulse facilitation is plotted against interpulse duration (Δ). The data were well fit with an exponential decay ($\tau = 27 \pm 2$ ms; $n = 5$ cells). The inset summarizes the voltage protocol. Error bars indicate SEM.

4). Under our recording conditions, reinhibition occurred with a time constant of 27 ± 2 ms, and was complete at intervals longer than $\sim$180 ms (Fig. 4B). Given that the interval between successive APW during a 5 Hz train is 200 ms, it is very unlikely that cumulative facilitation (summation) could occur.

To underscore this point, we stimulated cells with trains of APW applied at a frequency of 2.5 Hz (400 ms interval between successive APW). The decrease in amplitude of I_{Ca} during the 2.5 Hz train of APW (inactivation) was still significantly reduced by G-proteins (Fig. 5A,D). We also stimulated cells with a train of 75 APW applied at 25 Hz, a frequency at which a small degree of cumulative facilitation could occur (Currie and Fox, 2002). However, the effect of G-proteins on "inactivation" was no greater at 25 Hz (Fig. 5C), and showed no clear dependence on stimulation frequency (Fig. 5D). Together, these data (Figs. 4, 5) make it extremely unlikely that facilitation masks inactivation of I_{Ca} during the low-frequency stimulation used in this study.

Does reduced Ca^{2+} entry lead to reduced calcium-dependent inactivation?

Our data using 10 mM EGTA in the patch-pipette and/or extracellular Ba^{2+} show that VDI is reduced by G-proteins. However, our data suggest that CDI is also targeted, because the magnitude by which G-proteins reduce inactivation is greatest when CDI is intact (Fig. 2, 3). We have shown that CDI can be blocked by increasing the concentration of EGTA in the patch-pipette solution (Fig. 1B). Because EGTA will have little impact on the "local" domain of high Ca^{2+} near the mouth of an open channel (Naraghi and Neher, 1997), our data support the idea that a "global" elevation of cytosolic Ca^{2+} (influx through many channels) mediates CDI (Liang et al., 2003). Activation of G-proteins
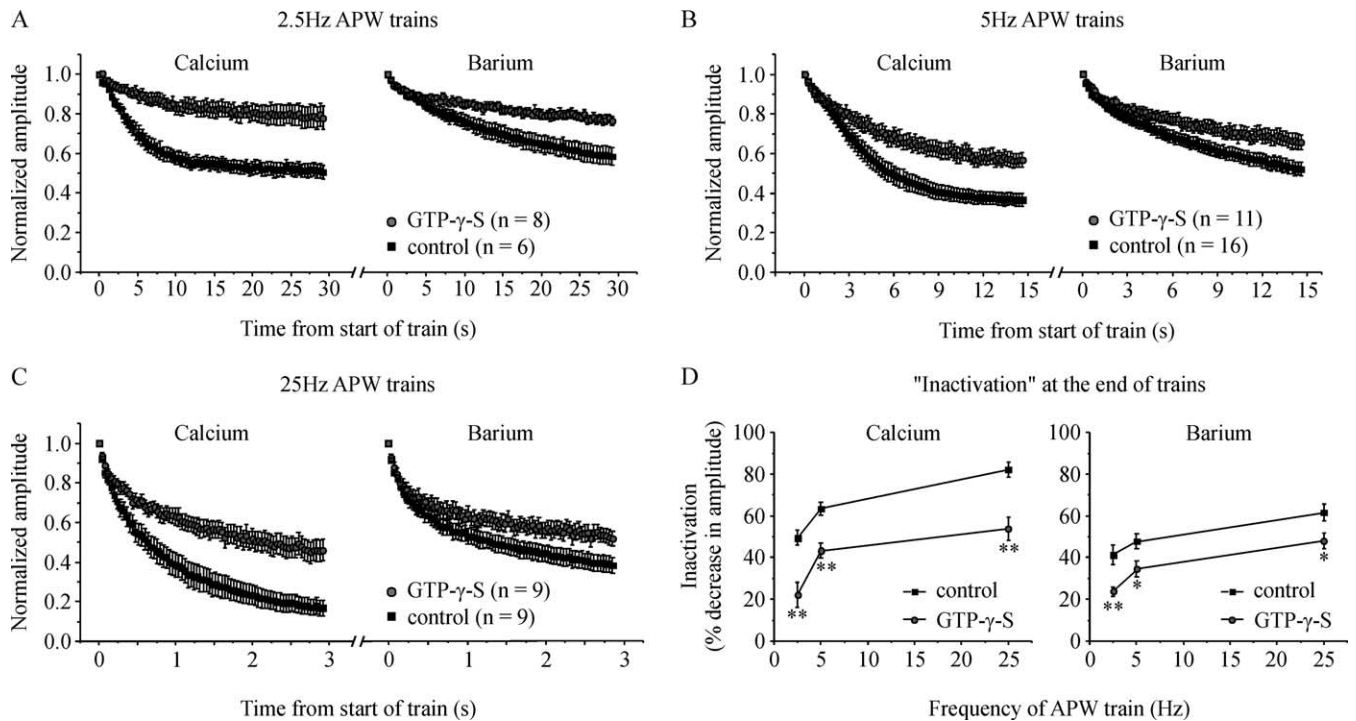
Figure 5. G-proteins reduce inactivation of I_{Ca} over a range of stimulation frequencies. Cells were stimulated with a train of 75 APW first in Ca^{2+}-containing extracellular solution and then in Ba^{2+}-containing extracellular solution. ***A–C***, Normalized current amplitude is plotted against time for cells stimulated at a frequency of: (***A***) 2.5 Hz, (***B***) 5 Hz (same data already shown in Fig. 2***C***), and (***C***) 25 Hz. ***D***, Mean inactivation (percent decrease in current amplitude at the end of the APW train) is plotted against stimulation frequency for control cells and cells with GTP-γ-S in the patch pipette to activate endogenous G-proteins. GTP-γ-S significantly reduced inactivation at all three stimulation frequencies in both Ca^{2+}-containing and Ba^{2+}-containing extracellular solution (*$p < 0.03$; **$p < 0.005$). Error bars indicate SEM.

reduces the amplitude of I_{Ca} compared with control conditions (Fig. 2*B*), so will presumably reduce the overall amount of Ca^{2+} entry into the cell. Could this decrease in Ca^{2+} entry result in reduced CDI during a train of APW?

To address this question we used two approaches to reduce the amplitude of I_{Ca}, and hence Ca^{2+} entry. First we used ω-conotoxin GVIA (Cgtx), a selective blocker of N-type Ca^{2+}-channels (Kasai et al., 1987; McCleskey et al., 1987). As illustrated in Figure 6*A*, a bolus of Cgtx (300 μl of 1 μM) was applied to the recording bath after the flow of extracellular solution was stopped. Block of I_{Ca} by Cgtx was relatively slow and was monitored by stimulating the cell once every 10 s with a single APW. When the amplitude of I_{Ca} was blocked by ~50–60% (1–2 min), the flow of solution through the bath was started to rapidly wash-out the Cgtx and prevent further channel block. Those channels already blocked remain blocked after wash-out because binding of Cgtx is essentially irreversible over this time course. The mean block of I_{Ca} amplitude was 58 ± 3%, which is similar in magnitude to the inhibition produced by G-proteins (Fig. 2*B*). We applied a train of APW (5 Hz for 15 s) before application of Cgtx and after washout of Cgtx. Inactivation of I_{Ca} was significantly reduced after Cgtx block (Fig. 6*B*, left). When the experiment was repeated with Ba^{2+}-containing extracellular solution, inactivation was not reduced (Fig. 6*B*, right), showing that Cgtx did not alter VDI. These data suggest that decreasing the number of "functional" Ca-channels (with Cgtx or during $G\beta\gamma$-mediated inhibition) reduces "global" Ca^{2+} entry and, hence, CDI.

In the second approach, we used a low concentration of $CdCl_2$ (~3 μM) to partially block I_{Ca} and reduce Ca^{2+} entry. Cells were stimulated with a train of APW first under control conditions and then during application of $CdCl_2$. Although Cd^{2+} blocked the peak amplitude of I_{Ca} by 40 ± 3% ($n = 6$), inactivation during a

5 Hz train of APW was not significantly altered in either Ca^{2+} or Ba^{2+} recording solutions (Fig. 6*C*). It is pertinent to note that Cgtx and Cd^{2+} block the channels by quite different mechanisms. Conotoxin will completely block those channels to which it is bound, whereas Ca^{2+} flux through unbound channels is left unaltered. Hence, this approach effectively reduces the number of functional channels but not Ca^{2+} flux through the channels per se. Channel blockade by low concentrations of Cd^{2+} is complex (Thevenod and Jones, 1992) and will alter Ca^{2+} flux through essentially all of the channels. Consistent with this view, we noted that the waveform of I_{Ca} elicited an APW was not altered by Cgtx but was slightly right-shifted by Cd^{2+} (Fig. 6*B,C*, insets).

Overall, our data underscore the complex nature of CDI, and show that some but not all manipulations that reduce overall Ca^{2+} entry can alter CDI. Hence, reduced CDI attributable to reduced Ca^{2+} entry is one plausible mechanism by which G-proteins might act, but this does not rule out other more direct effects on the conformational changes that underlie inactivation.

Subtle effects of G-proteins on voltage-dependent inactivation of I_{Ca}

Using Ba^{2+}-containing extracellular solution we show that VDI during a train of APW was reduced by GTP-γ-S and $G\beta\gamma$ (Figs. 2, 3, 5). Voltage-dependent inactivation of N-type I_{Ca} is complex and can occur from both open and closed-states of the channels. We examined the voltage-dependence of closed-state inactivation using the protocols illustrated in Figure 7*A*. All cells were recorded with Ba^{2+} rather than Ca^{2+} in the extracellular solution to rule out any possible contribution of CDI. In the first series of experiments, the holding potential was depolarized in increments of 10 mV once every 30 s. Progressive depolarization of the holding potential decreased the amplitude of I_{Ca} as more and
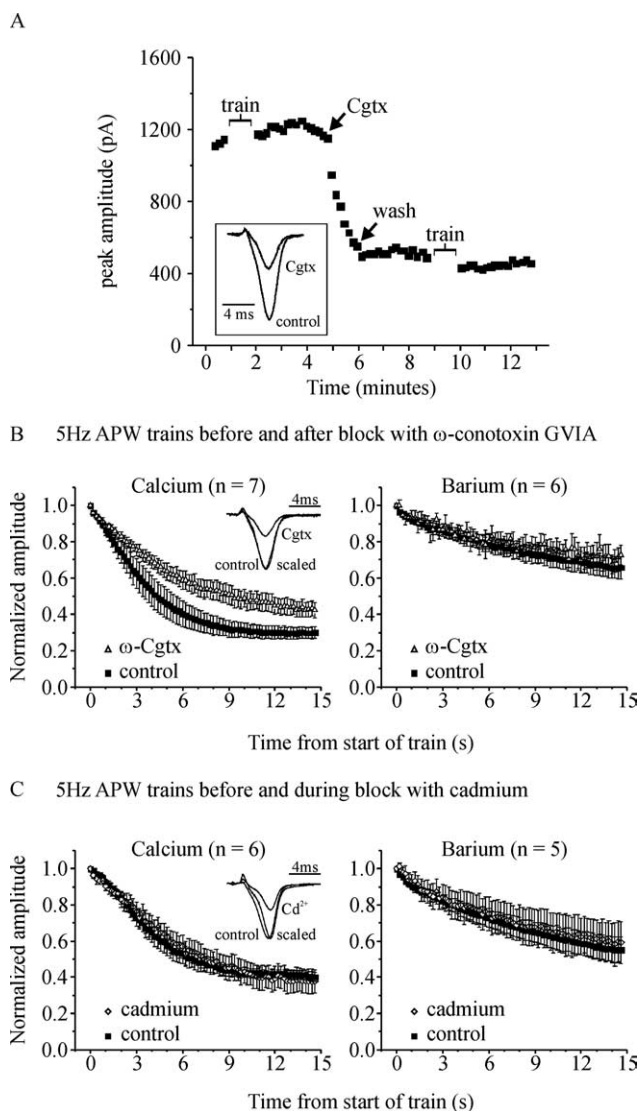
A

B   5Hz APW trains before and after block with ω-conotoxin GVIA

C   5Hz APW trains before and during block with cadmium

Figure 6. Evidence that reduced Ca^{2+} entry can lead to reduced calcium-dependent inactivation of I_{Ca}. **A**, Peak current amplitude elicited by an APW applied at 0.1 Hz is plotted against time from a representative cell to illustrate the experimental protocol. At the time indicated by the arrow labeled "Cgtx," the flow of solution through the recording bath was stopped and a bolus of ω-conotoxin GVIA (300 μl of 1 μM) was applied to the cells. When the amplitude of I_{Ca} was blocked by 50–60% (1–2 min), the flow of extracellular solution was restarted to rapidly wash away the Cgtx (arrow labeled "wash"). The cell was stimulated with a 5 Hz train of APW before and after Cgtx as indicated by the gaps in trace labeled "train." The inset shows representative I_{Ca} recorded before (control) and after Cgtx block. **B**, Left, Normalized peak amplitude of I_{Ca} during the 5 Hz APW trains is plotted against time. Cgtx significantly reduced inactivation of I_{Ca} during the train of APW ($p < 0.03; n = 7$). The inset shows currents from a representative cell; the current recorded before (control) and after application of Cgtx (Cgtx). The current recorded after Cgtx is also scaled to the same peak amplitude as control to show there was no shift in the waveform of I_{Ca} (scaled). The right panel shows that when Ca^{2+} was replaced with Ba^{2+} in the extracellular solution, block with Cgtx did not significantly change the inactivation of I_{Ba}. **C**, Same layout as **B** except that in these experiments trains of APW were applied before (control) and during continual perfusion of the cells with 3–5 μM $CdCl_2$ (cadmium). Cadmium blockade did not significantly alter inactivation in either Ca^{2+}- or Ba^{2+}-containing solutions. The inset shows that in addition to reducing the amplitude of I_{Ca}, Cd^{2+} produced a subtle but distinct shift in the waveform of I_{Ca} [the current recorded during Cd^{2+} blockade (scaled) is shifted to the right compared with control]. Error bars indicate SEM.

more of the channels became inactivated. With these 30 s conditioning pulses, inactivation was identical in control cells or in cells with GTP-γ-S in the patch-pipette solution [the potential at which 50% inactivation occurred ($V_{1/2}$) was −66 mV for control

cells and −67 mV for cells with GTP-γ-S]. However, when we used a 3 s conditioning pulse before activation of I_{Ba}, GTP-γ-S did significantly shift inactivation to more depolarized potentials [$V_{1/2} = −52 ± 1$ mV for control cells ($n = 4$) and −43 ± 2.6 mV for GTP-γ-S cells ($n = 5$); $p < 0.03$] (Fig. 7A).

We also investigated "closed-state" inactivation produced by depolarizing the holding potential to −60 mV for 2 min (Fig. 7B). Cells were stimulated with a 15 ms step depolarization to +10 mV once every 15 s (Fig. 7B) or once every 4 s (Fig. 7C) to monitor the onset and extent of inactivation. Cells that displayed excessive rundown (>10%) during a 2 min baseline period (at −100 mV holding potential) were excluded from analysis. Depolarizing the holding potential to −60 mV produced a reversible inactivation of I_{Ba}. Activation of endogenous G-proteins with GTP-γ-S had no effect on inactivation when cells were stimulated every 15 s (Fig. 7B,D). In contrast, GTP-γ-S produced a small but significant ($p < 0.04$) decrease in the extent of inactivation when cells were stimulated once every 4 s (Fig. 7C,D).

Overall, these data provide evidence that G-proteins can modulate closed-state, voltage-dependent inactivation, although these effects are subtle and show a critical dependence on the stimulation protocol.

Activation of P2Y purinergic receptors reduces inactivation of I_{Ca} in adrenal chromaffin cells

The above experiments used recombinant Ca-channels expressed in HEK293 cells, but we wanted to determine whether activation of endogenous G-protein-coupled receptors can modulate inactivation of I_{Ca} in a native cell type. We chose to use primary cultures of bovine adrenal chromaffin cells. Chromaffin cells are a well characterized neurosecretory model and, because of their small size and lack of neurites, they are readily voltage-clamped, an important consideration when using fast voltage commands that mimic action potentials. The Ca-channels in chromaffin cells are subject to voltage-dependent, Gβγ-mediated inhibition after activation of P2Y purinergic receptors (Albillos et al., 1996; Currie and Fox, 1996, 2002). Importantly, the P2Y receptors show little or no desensitization over several minutes (Currie and Fox, 1996). Furthermore, chromaffin cells typically fire at low frequencies (Brandt et al., 1976; Watkinson et al., 1990; Wallace et al., 2002) and the APW used in this study is based on an action potential recorded from a chromaffin cell at room temperature (Currie and Fox, 2002).

For these experiments we used amphotericin perforated whole-cell recordings to maintain the endogenous calcium buffering capacity of the cells (rather than using exogenous buffers like EGTA or BAPTA). Nitrendipine (a dihydropiridine antagonist) was included to prevent any possibility of activity-dependent recruitment of L-type Ca-channels (Artalejo et al., 1992) that could mask inactivation. Cells were stimulated with two trains of APW applied at 5 Hz for 15 s, first under control conditions and then during application of 10 μM ATP to activate the P2Y receptors. During the control train there was robust inactivation of I_{Ca} (56 ± 5% by the end of the train). After recovery, 10 μM ATP was applied to the cells and inhibited the peak amplitude of I_{Ca} by 47 ± 3% ($n = 5$) (Fig. 8A) as expected from previous work (Currie and Fox, 1996, 2002). ATP also significantly reduced the inactivation of I_{Ca} during the train of APW from 56 ± 5% in control conditions to 26 ± 4% with ATP present ($p < 0.003; n = 5$) (Fig. 8A,B). Consequently, during the APW train, the amplitude of I_{Ca} reached the same plateau level under control conditions and in the presence of ATP (Fig. 8A). Overall, these data corroborate our findings with recombinant channels,

increasing the likelihood that this effect could contribute to the regulation of calcium entry under physiological conditions.

Discussion

G-protein $\beta\gamma$ subunits reduce inactivation of N-type I_{Ca}

It is well established that G$\beta\gamma$ can bind directly to the α_1 subunit of N-type (Ca$_V$2.2) and P/Q-type (Ca$_V$2.1) Ca^{2+} channels (De Waard et al., 1997; Herlitze et al., 1997). This shifts the channels from "willing" to "reluctant" gating states, slows activation, and reduces the peak amplitude of whole-cell I_{Ca}. However, the effects of G$\beta\gamma$ on inactivation have remained unclear. One reason for this is the characteristic voltage-dependent reversal of G$\beta\gamma$-mediated inhibition. This reversal (facilitation) is most obvious after a strongly depolarizing prepulse (Figs. 2A, 4), but can also occur during steps to more modest membrane potentials like those commonly used to activate I_{Ca}. Facilitation masks the extent and kinetics of inactivation making it difficult to determine if these parameters are directly modulated by G-proteins.

We used trains of APW to activate I_{Ca} and more closely mimic physiological stimuli. Furthermore, low-frequency trains of APW circumvent the problem of facilitation which only occurs at higher-stimulation frequencies (see Results) (Fig. 4). We show that the amplitude of I_{Ca} undergoes substantial depression during trains of APW caused by voltage-dependent and calcium-dependent inactivation (Fig. 1). This depression was reduced by activation of endogenous G-proteins with GTP-γ-S, or expression of wild-type G$\beta\gamma$ in the HEK293 cells. The effect persisted at low-stimulation frequencies (2.5 Hz) (Fig. 5), making it very unlikely that facilitation was occurring and simply masking inactivation. Therefore, we propose that G$\beta\gamma$ produces a genuine decrease in the inactivation of I_{Ca}. We also demonstrate the same phenomenon in adrenal chromaffin cells, where inactivation of I_{Ca} was reduced by endogenous P2Y purinergic receptors (Fig. 8).

Ca^{2+}-dependent inactivation of I_{Ca}

CDI played a significant role during trains of APW, although the onset was relatively slow compared with VDI (Fig. 1). Increasing the concentration of EGTA in the patch-pipette solution from 0.3 to 10 mM (Fig. 1B) abolished CDI, as did 5 mM BAPTA. EGTA will have little impact on the "local" microdomain of high Ca^{2+} near to the mouth of an open channel, suggesting that CDI is mediated by a more "global" elevation of intracellular Ca^{2+} because of influx through many channels (Liang et al., 2003). We also noted that with 10 mM EGTA, the depression of I_{Ca} during a train of APW was actually less in Ca^{2+} than in Ba^{2+} (Fig. 1B, right). Perhaps 10 mM EGTA unmasks a small, slowly developing,
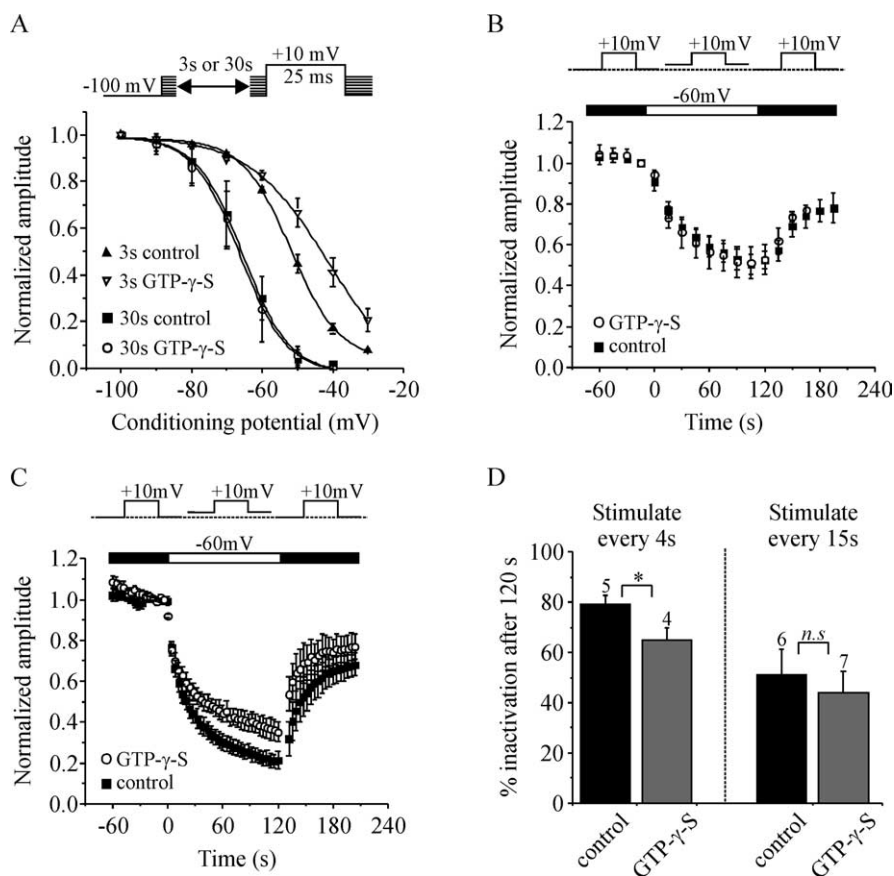

Figure 7. G-proteins have subtle effects on closed-state inactivation of I_{Ca}. **A**, Plots of the voltage dependence of closed-state inactivation. Cells were recorded with Ba^{2+}-containing extracellular solution. The top illustrates the experimental protocols. A conditioning pulse to various potentials (-100 mV to -30 mV) was applied for either 30 or 3 s before activation of I_{Ba}. Current amplitude was normalized, plotted against the potential of the conditioning pulse, and the mean data fit with a Boltzman curve. When a 30 s conditioning pulse was used, GTP-γ-S had no effect on the inactivation curve. However, when a 3 s conditioning pulse was used, GTP-γ-S significantly shifted the inactivation curve by $\sim$9 mV in the depolarizing direction ($V_{1/2} = -52 \pm 1$ mV, $n = 4$ vs -43 ± 2.6 mV, $n = 5$; $p < 0.03$). **B**, Normalized I_{Ba} amplitude is plotted against time and the insert (above) illustrates the experimental protocol. Cells were stimulated by a 15 ms test pulse to $+10$ mV applied once every 15 s. Depolarizing the holding potential to -60 mV (from -100 mV or from -80 mV as shown) produced a reversible inactivation of I_{Ba}. GTP-γ-S did not significantly alter this inactivation. **C**, The same layout as in **B** except that cells were stimulated once every 4 s rather than once every 15 s. GTP-γ-S reduced the inactivation produced by changing the holding potential to -60 mV. **D**, Plots the mean inactivation (percent decrease in current amplitude) 120 s after changing the holding potential to -60 mV in cells stimulated once every 4 s (as in **C**), or once every 15 s (as **B**). *$p < 0.04$; n.s., Not statistically significant. Error bars indicate SEM.

Ca^{2+}-dependent facilitation, although this was not apparent with BAPTA and was not investigated further in this study.

When examining the effects of G-proteins on inactivation, two things were immediately apparent. First, inactivation was reduced in Ba^{2+}-containing solutions, indicating that VDI was targeted. Second, the magnitude of the decrease produced by G-proteins was greater in Ca^{2+} than in Ba^{2+}, suggesting that CDI was also targeted (Figs. 2B, 3B, 5). Given that G-proteins reduced the amplitude of I_{Ca} by $\sim$50%, we reasoned that, in turn, the reduced Ca^{2+} entry might lead to reduced CDI. Consistent with this idea, partially blocking I_{Ca} with ω-conotoxin GVIA reduced inactivation during a train of APW (Fig. 6B). This effect was on CDI not VDI, because Cgtx did not alter inactivation in Ba^{2+}-containing solution. However, when we used low-concentrations of Cd^{2+} to partially block I_{Ca}, there was no effect on inactivation (Fig. 6C). We considered the possibility that Cd^{2+} itself was accelerating inactivation and thereby masking the effect of decreased Ca^{2+} entry, but this seems unlikely because Cd^{2+} did not alter inactivation in Ba^{2+}-containing solution.
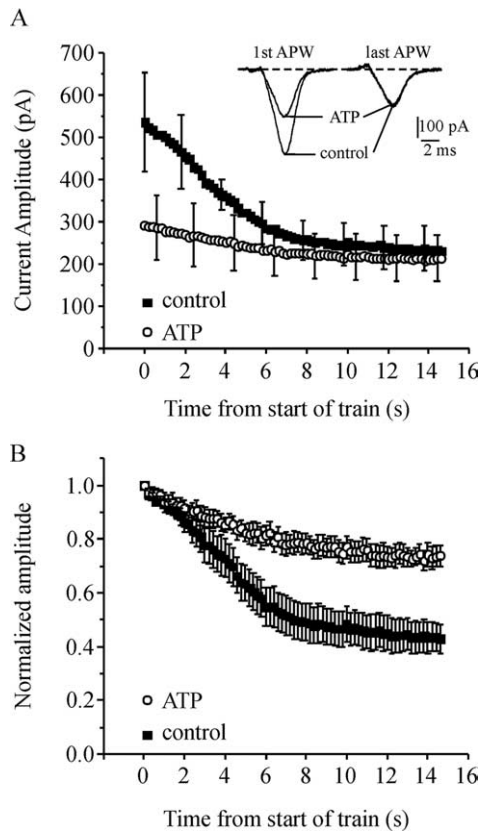
A

B

Figure 8. Activation of endogenous P2Y purinergic receptors reduces inactivation of I_{Ca} in bovine adrenal chromaffin cells. Chromaffin cells were recorded using the amphotericin perforated whole-cell recording configuration to maintain endogenous calcium buffers. The cells were stimulated with a 5 Hz train of APW lasting 15 s first under control conditions and then in the presence of 10 μM extracellular ATP. ATP activates P2Y receptors to produce G$\beta\gamma$-mediated inhibition of I_{Ca}. The extracellular solution contained 2 mM Ca^{2+} in these experiments. **A**, Mean peak amplitude of I_{Ca} under control conditions and in the presence of ATP is plotted against time for the duration of the APW train ($n = 5$). The inset shows four currents from a representative cell. These currents were elicited by the first and last APW of the train under control conditions and in the presence of ATP. (Note that for display clarity, error bars are not shown for every data point.) **B**, The same data as in **A** except the amplitude of I_{Ca} is normalized to the first pulse within each train. ATP significantly reduced inactivation during the train of APW ($p < 0.003$). Error bars indicate SEM.

Why might Cgtx and Cd^{2+} have different effects on CDI? It is worth noting that the two blockers work by quite different mechanisms. Channel blockade by Cd^{2+} is complex (Thevenod and Jones, 1992) and will result in altered Ca^{2+} flux through all of the channels. In contrast, Cgtx will completely block those channels to which it is bound, whereas Ca^{2+} flux through unbound channels is left unaltered. This difference is manifest in the waveform of I_{Ca}, which is unaltered by Cgtx but right-shifted by Cd^{2+} (Fig. 6B,C). Therefore, it is conceivable that the two blockers have quite different effects on intracellular Ca^{2+} dynamics, although additional work is needed to address this. Arguably, the effect of G$\beta\gamma$ on Ca^{2+} entry is more closely mimicked by Cgtx than by Cd^{2+}. Although G$\beta\gamma$-bound "reluctant" channels display low-probability openings with submillisecond open times, the most noticeable effect of G$\beta\gamma$ is to increase the latency to first channel opening (Carabelli et al., 1996; Patil et al., 1996; Lee and Elmslie, 2000; Colecraft et al., 2001). In the context of a brief APW, the major effect will be to decrease the number of Ca-channels that open, with only small effects on Ca^{2+} flux per se.

These data underscore the complex nature of CDI and show

that not all manipulations that change Ca^{2+} entry impact CDI. In the context of this study, we propose that reduced CDI attributable to reduced Ca^{2+} entry is one plausible mechanism by which G-proteins can modulate I_{Ca}. However, it is also possible that G$\beta\gamma$ has a more direct effect by interfering with the conformational changes that underlie CDI.

Voltage-dependent inactivation of I_{Ca}
VDI of N-type Ca-channels can occur from both open and closed states. During repetitive stimuli, the channels preferentially inactivate from intermediate closed state(s), and it has been postulated that G$\beta\gamma$ could increase the probability that the Ca-channels occupy these states and thereby accelerate inactivation (Patil et al., 1998). However, our data show that VDI was reduced, not accelerated, by G-proteins (Figs. 2, 3,5). Perhaps G$\beta\gamma$ decreases the probability that the channels populate the particular closed-state from which inactivation is maximal. In addition, we show that the voltage-dependence of closed-state inactivation was shifted to more depolarized potentials by G-proteins (Fig. 7A). This shift was apparent when 3 s conditioning pulses were used to produce inactivation, but not when 30 s conditioning pulses were used (Fig. 7A). A similar difference is seen in a study comparing splice variants of $Ca_V2.2$; short conditioning pulses revealed a shift in the voltage dependence of closed-state inactivation, whereas longer conditioning pulses showed no shift (Thaler et al., 2004). Perhaps longer conditioning pulses overcome the effect of G$\beta\gamma$, or recruit an additional slow component to closed-state inactivation that is insensitive to G$\beta\gamma$.

We also investigated VDI produced by a modest depolarization of the resting membrane potential (Fig. 7). Cells stimulated once every 4 s showed robust inactivation when the holding potential was depolarized to -60 mV, and this was significantly reduced by G-protein activation (Fig. 7C). However, when cells were stimulated once every 15 s, the same shift in holding potential produced less inactivation in control cells, and G-protein activation had no effect (Fig. 7B,D). It is possible that more frequent stimulation favors inactivation from a particular closed state of the channel, or the accumulation of inactivation from open-channel states. Nevertheless, our data show that G-proteins can exert subtle modulatory effects on VDI and suggest that at least some of these effects might be on closed-state inactivation.

The molecular mechanisms that underlie inactivation of Ca-channels remain unclear. Fast VDI might involve a "hinged lid"-type mechanism, with the intracellular loop connecting domains I and II of the Ca-channel α_1 subunit serving as the "inactivation gate" (Restituito et al., 2000; Stotz et al., 2000; Stotz and Zamponi, 2001; Geib et al., 2002; Cens et al., 2006). Intriguingly, the I–II loop is also a primary binding site of G$\beta\gamma$ on the Ca-channel (De Waard et al., 1997, 2005; Herlitze et al., 1997). This raises the possibility that binding of G$\beta\gamma$ disrupts movement of this putative inactivation gate, or its interaction with other channel domains. We show that W332A-G$\beta\gamma$, a point mutant with reduced affinity for the Ca-channel (Agler et al., 2003), has no effect on inactivation, consistent with the idea that G$\beta\gamma$ must bind to the channel to produce its effects (Fig. 3). Future work will investigate this possible mechanism.

Physiological implications
We show that G$\beta\gamma$ reduces inactivation of I_{Ca}, and thereby alters the temporal profile as well as the absolute amount of Ca^{2+} influx during a train of APW. In turn, this could influence the accumulation of intracellular Ca^{2+} and Ca^{2+}-dependent events such as neurotransmitter and hormone release. However, an important

caveat is that our experiments were performed at room temperature, and it is difficult to predict the combined effects of raising the temperature on channel gating, calcium handling, and G-protein signaling. It is also notable that reduced inactivation confers a temporal component to the inhibition of I_{Ca} amplitude by G$\beta\gamma$. With sustained trains of APW, the amplitude of I_{Ca} elicited by each APW converges under control and G$\beta\gamma$-modulated conditions (Figs. 2B, 8A). It is already known that brief high-frequency bursts of APW can partially relieve G$\beta\gamma$ binding to Ca-channels and thereby enhance Ca^{2+} entry (facilitation). Our data suggest that sustained low-frequency firing can also significantly reduce the "efficacy" of G$\beta\gamma$-mediated inhibition. Future experiments will investigate how tonic versus burst firing impacts G$\beta\gamma$-mediated regulation of I_{Ca} and transmitter release.

References

Agler HL, Evans J, Colecraft HM, Yue DT (2003) Custom distinctions in the interaction of G-protein beta subunits with N-type (Ca$_V$2.2) versus P/Q-type (Ca$_V$2.1) calcium channels. J Gen Physiol 121:495–510.

Albillos A, Gandia L, Michelena P, Gilabert JA, del Valle M, Carbone E, Garcia AG (1996) The mechanism of calcium channel facilitation in bovine chromaffin cells. J Physiol (Lond) 494:687–695.

Artalejo CR, Rossie S, Perlman RL, Fox AP (1992) Voltage-dependent phosphorylation may recruit Ca^{2+} current facilitation in chromaffin cells. Nature 358:63–66.

Bean BP (1989) Neurotransmitter inhibition of neuronal calcium currents by changes in channel voltage dependence. Nature 340:153–156.

Boland LM, Bean BP (1993) Modulation of N-type calcium channels in bullfrog sympathetic neurons by luteinizing hormone-releasing hormone: kinetics and voltage dependence. J Neurosci 13:516–533.

Brandt BL, Hagiwara S, Kidokoro Y, Miyazaki S (1976) Action potentials in the rat chromaffin cell and effects of acetylcholine. J Physiol (Lond) 263:417–439.

Brody DL, Patil PG, Mulle JG, Snutch TP, Yue DT (1997) Bursts of action potential waveforms relieve G-protein inhibition of recombinant P/Q-type Ca^{2+} channels in HEK 293 cells. J Physiol (Lond) 499:637–644.

Carabelli V, Lovallo M, Magnelli V, Zucker H, Carbone E (1996) Voltage-dependent modulation of single N-Type Ca^{2+} channel kinetics by receptor agonists in IMR32 cells. Biophys J 70:2144–2154.

Cens T, Rousset M, Leyris JP, Fesquet P, Charnet P (2006) Voltage- and calcium-dependent inactivation in high voltage-gated Ca(2+) channels. Prog Biophys Mol Biol 90:104–117.

Colecraft HM, Patil PG, Yue DT (2000) Differential occurrence of reluctant openings in G-protein-inhibited N- and P/Q-type calcium channels. J Gen Physiol 115:175–192.

Colecraft HM, Brody DL, Yue DT (2001) G-protein inhibition of N- and P/Q-type calcium channels: distinctive elementary mechanisms and their functional impact. J Neurosci 21:1137–1147.

Cox DH, Dunlap K (1994) Inactivation of N-type calcium current in chick sensory neurons: calcium and voltage dependence. J Gen Physiol 104:311–336.

Currie KP, Fox AP (1996) ATP serves as a negative feedback inhibitor of voltage-gated Ca^{2+} channel currents in cultured bovine adrenal chromaffin cells. Neuron 16:1027–1036.

Currie KP, Fox AP (2002) Differential facilitation of N- and P/Q-type calcium channels during trains of action potential-like waveforms. J Physiol (Lond) 539:419–431.

De Waard M, Liu H, Walker D, Scott VE, Gurnett CA, Campbell KP (1997) Direct binding of G-protein $\beta\gamma$ complex to voltage-dependent calcium channels. Nature 385:446–450.

De Waard M, Hering J, Weiss N, Feltz A (2005) How do G proteins directly control neuronal Ca^{2+} channel function? Trends Pharmacol Sci 26:427–436.

Dolphin AC (2003) G protein modulation of voltage-gated calcium channels. Pharmacol Rev 55:607–627.

Elmslie KS (2003) Neurotransmitter modulation of neuronal calcium channels. J Bioenerg Biomembr 35:477–489.

Elmslie KS, Zhou W, Jones SW (1990) LHRH and GTP-gamma-S modify

calcium current activation in bullfrog sympathetic neurons. Neuron 5:75–80.

Fenwick EM, Fajdiga PB, Howe NB, Livett BG (1978) Functional and morphological characterization of isolated bovine adrenal medullary cells. J Cell Biol 76:12–30.

Ford CE, Skiba NP, Bae H, Daaka Y, Reuveny E, Shekter LR, Rosal R, Weng G, Yang CS, Iyengar R, Miller RJ, Jan LY, Lefkowitz RJ, Hamm HE (1998) Molecular basis for interactions of G protein betagamma subunits with effectors. Science 280:1271–1274.

Geib S, Sandoz G, Cornet V, Mabrouk K, Fund-Saunier O, Bichet D, Villaz M, Hoshi T, Sabatier JM, De Waard M (2002) The interaction between the I-II loop and the III-IV loop of Cav2.1 contributes to voltage-dependent inactivation in a beta -dependent manner. J Biol Chem 277:10003–10013.

Golard A, Siegelbaum SA (1993) Kinetic basis for the voltage-dependent inhibition of N-type calcium current by somatostatin and norepinephrine in chick sympathetic neurons. J Neurosci 13:3884–3894.

Goo YS, Lim W, Elmslie KS (2006) Ca2+ enhances U-type inactivation of N-type (Ca$_V$2.2) calcium current in rat sympathetic neurons. J Neurophysiol.

Greenberg A, Zinder O (1982) Alpha- and beta-receptor control of catecholamine secretion from isolated adrenal medulla cells. Cell Tissue Res 226:655–665.

Herlitze S, Hockerman GH, Scheuer T, Catterall WA (1997) Molecular determinants of inactivation and G protein modulation in the intracellular loop connecting domains I and II of the calcium channel αA subunit. Proc Natl Acad Sci USA 94:1512–1516.

Ikeda SR, Dunlap K (1999) Voltage-dependent modulation of N-type calcium channels: role of G protein subunits. Adv Second Messenger Phosphoprotein Res 33:131–151.

Jones SW, Marks TN (1989) Calcium currents in bullfrog sympathetic neurons. II. Inactivation. J Gen Physiol 94:169–182.

Kasai H, Aosaki T, Fukuda J (1987) Presynaptic Ca-antagonist omega-conotoxin irreversibly blocks N-type Ca channels in chick sensory neurons. Neurosci Res 4:228–235.

Lee HK, Elmslie KS (2000) Reluctant gating of single N-type calcium channels during neurotransmitter-induced inhibition in bullfrog sympathetic neurons. J Neurosci 20:3115–3128.

Liang H, Elmslie KS (2001) E(f)- current contributes to whole-cell calcium current in low calcium in frog sympathetic neurons. J Neurophysiol 86:1156–1163.

Liang H, DeMaria CD, Erickson MG, Mori MX, Alseikhan BA, Yue DT (2003) Unified mechanisms of Ca^{2+} regulation across the Ca^{2+} channel family. Neuron 39:951–960.

McCleskey EW, Fox AP, Feldman DH, Cruz LJ, Olivera BM, Tsien RW, Yoshikami D (1987) Omega-conotoxin: direct and persistent blockade of specific types of calcium channels in neurons but not muscle. Proc Natl Acad Sci USA 84:4327–4331.

McCool BA, Pin JP, Brust PF, Harpold MM, Lovinger DM (1996) Functional coupling of rat group II metabotropic glutamate receptors to an omega-conotoxin GVIA-sensitive calcium channel in human embryonic kidney 293 cells. Mol Pharmacol 50:912–922.

McCool BA, Pin JP, Harpold MM, Brust PF, Stauderman KA, Lovinger DM (1998) Rat group I metabotropic glutamate receptors inhibit neuronal Ca^{2+} channels via multiple signal transduction pathways in HEK 293 cells. J Neurophysiol 79:379–391.

Meir A, Dolphin AC (2002) Kinetics and G$\beta\gamma$ modulation of Ca(v)2.2 channels with different auxiliary beta subunits. Pflugers Arch 444:263–275.

Naraghi M, Neher E (1997) Linearized buffered Ca^{2+} diffusion in microdomains and its implications for calculation of [Ca^{2+}] at the mouth of a calcium channel. J Neurosci 17:6961–6973.

Park D, Dunlap K (1998) Dynamic regulation of calcium influx by G-proteins, action potential waveform, and neuronal firing frequency. J Neurosci 18:6757–6766.

Patil PG, de Leon M, Reed RR, Dubel S, Snutch TP, Yue DT (1996) Elementary events underlying voltage-dependent G-protein inhibition of N-type calcium channels. Biophys J 71:2509–2521.

Patil PG, Brody DL, Yue DT (1998) Preferential closed-state inactivation of neuronal calcium channels. Neuron 20:1027–1038.

Penington NJ, Kelly JS, Fox AP (1991) A study of the mechanism of Ca^{2+} current inhibition produced by serotonin in rat dorsal raphe neurons. J Neurosci 11:3594–3609.

Restituito S, Cens T, Barrere C, Geib S, Galas S, De Waard M, Charnet P (2000) The β2a subunit is a molecular groom for the Ca^{2+} channel inactivation gate. J Neurosci 20:9046–9052.

Stotz SC, Zamponi GW (2001) Structural determinants of fast inactivation of high voltage-activated Ca(2+) channels. Trends Neurosci 24:176–181.

Stotz SC, Hamid J, Spaetgens RL, Jarvis SE, Zamponi GW (2000) Fast inactivation of voltage-dependent calcium channels. A hinged-lid mechanism? J Biol Chem 275:24575–24582.

Thaler C, Gray AC, Lipscombe D (2004) Cumulative inactivation of N-type $Ca_V2.2$ calcium channels modified by alternative splicing. Proc Natl Acad Sci USA 101:5675–5679.

Thevenod F, Jones SW (1992) Cadmium block of calcium current in frog sympathetic neurons. Biophys J 63:162–168.

Tosetti P, Taglietti V, Toselli M (1999) Action-potential-like depolarizations relieve opioid inhibition of N-type Ca^{2+} channels in NG108–15 cells. Pflugers Arch 437:441–448.

Wallace DJ, Chen C, Marley PD (2002) Histamine promotes excitability in bovine adrenal chromaffin cells by inhibiting an M-current. J Physiol (Lond) 540:921–939.

Watkinson A, O'Sullivan AJ, Burgoyne RD, Dockray GJ (1990) Differential accumulation of catecholamines, proenkephalin- and chromogranin A-derived peptides in the medium after chronic nicotine stimulation of cultured bovine adrenal chromaffin cells. Peptides 11:435–441.

Williams S, Serafin M, Muhlethaler M, Bernheim L (1997) Facilitation of N-type calcium current is dependent on the frequency of action potential-like depolarizations in dissociated cholinergic basal forebrain neurons of the guinea pig. J Neurosci 17:1625–1632.

Womack MD, McCleskey EW (1995) Interaction of opioids and membrane potential to modulate Ca^{2+} channels in rat dorsal root ganglion neurons. J Neurophysiol 73:1793–1798.

Yasuda T, Chen L, Barr W, McRory JE, Lewis RJ, Adams DJ, Zamponi GW (2004) Auxiliary subunit regulation of high-voltage activated calcium channels expressed in mammalian cells. Eur J Neurosci 20:1–13.